

Analysis of transient processes in a susceptible motion transmission pump drive system with asynchronous motor

Abstract. The paper presents mathematical model of the hydraulic system using the generalized variation method. The hydraulic system consists of a power transformer, capacitor banks and deep-bar asynchronous pump drives with susceptible movement transmission. The element of motion transmission is a flexible coupling with mechanical lumped parameters. On the base of the developed model, electromechanical transient processes in the drive system are analyzed. The final system state equations are presented in the normal form of Cauchy. The equations are solved using hidden numerical methods. The results of the computer simulation are presented in graphic form.

Streszczenie. W pracy, wykorzystując uogólnioną metodę wariacyjną zaproponowano model matematyczny układu hydraulicznego, który składa się z transformatora mocy, baterii kondensatorów oraz głębokożłobkowych asynchronicznych napędów pompowych o podatnej transmisji ruchu. Elementem transmisji ruchu jest sprzęgło elastyczne o mechanicznych parametrach skupionych. Na podstawie opracowanego modelu analizuje się elektromechaniczne procesy niustalone w układzie napędowym. Końcowe równania stanu systemu przedstawione są w normalnej postaci Cauchy'ego i są rozwiązywane za pomocą ukrytych metod numerycznych. Wyniki symulacji komputerowej przedstawiono w postaci graficznej. (Analiza procesów niustalonych w pompowym układzie napędowym z silnikiem asynchronicznym o podatnej transmisji ruchu).

Keywords: interdisciplinary variation method, hydraulic system, electromechanical unit, deep-bar asynchronous motor, compensating capacitor bank, flexible coupling, flexible movement transmission.

Słowa kluczowe: interdyscyplinarna metoda wariacyjna, układ hydrauliczny, zespół elektromechaniczny, głębokożłobkowy silnik asynchroniczny, kompensacyjna bateria kondensatorów, sprzęgło elastyczne, podatna transmisja ruchu.

Introduction

Electromechanical drives take important place in the national economy. This is because the electromechanical drives execution of various types of complicated tasks, including hydraulic systems with vertical pumps [3], [4], [5], [7], [9].

In most cases, several pumps should be used to perform the tasks performed by the hydraulic system. Movement transmission of asynchronous pumping systems is complicated. The pump set transient states effective analysis requires mechanical sub-system consideration as susceptible system. The transient analysis can be performed as the case of transmissions with lumped parameters or transmission with distributed parameters. Modeling methods are significantly differing in both cases. An important element in modeling the hydraulic system is possibility to divide into two parts. In the first part there is no compensating battery and there are no units which would not comprise battery. The part is presented in figure 1.

In this paper, the hydraulic unit mathematical model based on the interdisciplinary variational method [1] is created. This model consists of a vertical pump which is coupled with a deep-bar asynchronous motor with susceptible movement transmission. The movement transmission is implemented on the base of flexible elastic-dissipative clutch with mechanical lumped parameters. The clutch transmits torque from the motor to vertical pump blades.

The listed drives are parts of the electric unit. The electric unit cooperating with the reactive power compensation battery in the power system. In this case, the transient state processes are analyzed in the electro-hydraulic-mechanical unit. This is the main goal of this work.

The mathematical model of system

In the general case, M drives are considered - figure 1. The mathematical model of the system uses the variation method presented in [1].

The variation of the functional activities should be determined and equate it to zero to obtain a mathematical model of the object [1], [10], [12].

$$(1) \quad \delta S = \delta \int_0^{t_1} L^* dt = \int_0^{t_1} \delta L^* dt = \int_0^{t_1} \left(\frac{\partial L^*}{\partial q_i} \delta q_i + \frac{\partial L^*}{\partial \dot{q}_i} \delta \dot{q}_i \right) dt = 0$$

As a result, the Euler-Lagrange or Euler-Poisson equations for systems with distributed parameters are obtained. The mathematical model of the system model will include these equations.

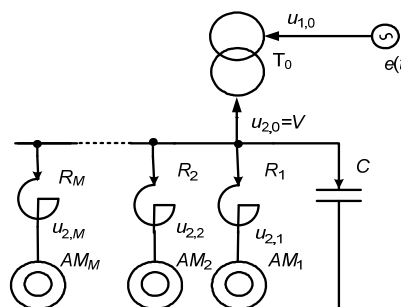


Fig. 1. The electrical unit basic diagram

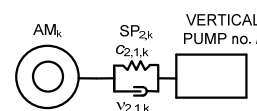


Fig. 2. Mechanical basic diagram of the k pump system

The following generalized coordinates of the system are introduced:

- for a power transformer: $q_{(1-6)} = Q_{1A}, Q_{1B}, Q_{1C}, Q_{2A}, Q_{2B}, Q_{2C}$ – primary and secondary windings electric charge;
- for stators and rotors of asynchronous motors: $q_{(7-12),k} = Q_{SA,k}, Q_{SB,k}, Q_{SC,k}, Q_{RA,k}, Q_{RB,k}, Q_{RC,k}$ – stator S and rotor R windings electric charge;
- for the movement transmission: $q_{13,k} = \gamma_{1,k}$ – rotation angle of the motor rotor, $q_{14,k} = \gamma_{2,k}$ – angle of rotation of the pump rotor,
- $q_{15,k} = V_k$ – pump flow; $q_{(16-18)} = Q_{CA}, Q_{CB}, Q_{CC}$ – the capacitor bank electric charge.

The currents values, pumps flows and rotors angular speeds are determined taking into account generalized speeds $\dot{q} \equiv dq/dt$. $\dot{q}_{(1-12),k} = i_{j,k}$ – currents of transformer and motors winding, $\dot{q}_{13,k}, \dot{q}_{14,k} = \omega_{1,k}, \omega_{2,k}$ – motors and pumps angular speeds, $\dot{q}_{15,k} = Q_k$ – pumps flow, $\dot{q}_{(16-18)} = i_{CA}, i_{CB}, i_{CC}$ – capacitor bank currents.

All parameters and functional dependencies of the transformer and asynchronous motor have been reduced to the secondary winding of the transformer and to the stator winding.

The elements of non-conservative forces in Lagrangian for the power system (fig. 1) are described with equations [1], [2], [6], [8]:

$$(2) \quad \tilde{T}^* \equiv \tilde{T}_{TM}^* + \left[\sum_{k=1}^M \tilde{T}_{AM,k}^* \right] + \left[\sum_{k=1}^M \tilde{T}_{X,k}^* \right] + \left[\sum_{k=1}^M \tilde{T}_{SP,k}^* \right] + \left[\sum_{k=1}^M \tilde{T}_{P,k}^* \right] =$$

$$= \sum_{j=1}^3 \left[\int_0^{i_{1j}} \Psi_{1j} di_{1j} + \int_0^{i_{2j}} \Psi_{2j} di_{2j} \right] + \sum_{k=1}^M \left\{ \sum_{j=1}^3 \int_0^{i_{Sj,k}} \Psi_{Sj,k} di_{Sj,k} + \right.$$

$$+ \int_0^{i_{Rj,k}} \Psi_{Rj,k} di_{Rj,k} \left. \right\} + \left[\sum_{j=1}^3 \frac{L_{X,k} i_{Sj,k}^2}{2} \right] + \left[\frac{J_{1,k} \omega_{1,k}^2}{2} + \frac{J_{2,k} \omega_{2,k}^2}{2} \right] + \left[\frac{L_{\Sigma,k} Q_k^2}{2} \right], \quad J_{1,k} \equiv J_{EM,k}, \quad J_{2,k} \equiv J_{P,k};$$

$$(3) \quad P^* = \sum_{j=1}^3 \left[\frac{Q_{Cj}^2}{2C} \right] + \sum_{k=1}^M \left[\frac{c_{1,2,k} (\gamma_{2,k} - \gamma_{1,k})}{2} \right];$$

$$(4) \quad \Phi = \sum_{j=1}^3 \frac{1}{2} \left[\int_0^t r_{1j,k} i_{1j,k}^2 d\tau + \int_0^t r_{2j,k} i_{2j,k}^2 d\tau \right] + \sum_{k=1}^M \left\{ \sum_{j=1}^3 \frac{1}{2} \left[\int_0^t r_{Sj,k} i_{Sj,k}^2 d\tau + \int_0^t r_{RLj,k} i_{Rj,k}^2 d\tau \right] + \left[\frac{v_{1,2,k} (\omega_{2,k} - \omega_{1,k})}{2} \right] + \frac{1}{2} \int_0^t R_{\Sigma,k} Q_k^2 d\tau \right\}, \quad j = A, B, C;$$

$$(5) \quad D^* = \int_0^t (e_A i_{1A} + e_B i_{1B} + e_C i_{1C}) d\tau - \sum_{k=1}^M \int_0^t \int_0^{\omega_{2,k}} M_{P,k} (\omega_{2,k}) d\omega_{2,k} d\tau;$$

where individual indices refer to: *TM* – power transformer, *AM* – asynchronous motor, *X* – air-core coil, *SP* – clutch, *P* – pumping system: pump and pipeline;

Ψ – column vectors of full transformer and motor magnetic flux; \mathbf{r} – transformer windings resistance matrix, for stator *S* and front part of rotor *RL*; \mathbf{i} – column vectors of currents, \mathbf{u} – column vectors of transformer supply voltage; c, v – coefficient of rigidity and dispersion of the clutch, J – moment of inertia, R_{Σ}, L_{Σ} – virtual resistance and inductance of pump system, C – compensation battery capacity, e – electromotive force.

The following assumptions were accepted using the White and Woodson theory [1], [12]:

$$(6) \quad u_{2j} = \frac{\partial [\tilde{T}_{TM}^*]}{\partial Q_{2j}}, \quad M_{EM,k} = \frac{\partial [\tilde{T}_{AM,k}^*]}{\partial \gamma_{1,k}}, \quad u_{RLj,k} = -\frac{\partial [\tilde{T}_{AM,k}^*]}{\partial Q_{Rj,k}},$$

$$\rho_{H,k} g (H_{G,k} + S_{0,k} Q_k^2) = \frac{\partial [\tilde{T}_{\Sigma,k}^*]}{\partial V_k}, \quad k = 1, 2, \dots, M$$

where: u_2 – power supply voltage of the power transformer secondary winding, M_{EM} – motor starting torque, u_{RL} – the cage bars voltage of asynchronous motor, ρ_H – fluid density, g – earth acceleration, H_G – liquid height, S_0 – hydraulic resistance of pipeline.

Substituting the expressions (2) – (5) in (1) and taking into account (6), then recalculated magnetic flux coordinates model Ψ -type to current coordinates model A -type [1] the object state equations are as follows:

$$(7) \quad \frac{d\mathbf{i}_1}{dt} = \mathbf{A}_{11} (\mathbf{e} - \mathbf{r}_1 \mathbf{i}_1) + \mathbf{A}_{12} (\mathbf{V} - \mathbf{r}_2 \mathbf{i}_2);$$

$$(8) \quad \frac{d\mathbf{i}_2}{dt} = \mathbf{A}_{21} (\mathbf{e} - \mathbf{r}_1 \mathbf{i}_1) + \mathbf{A}_{22} (\mathbf{V} - \mathbf{r}_2 \mathbf{i}_2);$$

$$(9) \quad \frac{d\mathbf{i}_{X,k}}{dt} = \alpha_{X,k} (\mathbf{V} - \mathbf{u}_{S,k} - R_{X,k} \mathbf{i}_{S,k}), \quad \alpha_{X,k} = \frac{1}{L_{X,k}};$$

$$(10) \quad \frac{d\mathbf{i}_{S,k}}{dt} = \mathbf{A}_{S,k} (\mathbf{u}_{S,k} - \mathbf{r}_{S,k} \mathbf{i}_{S,k}) + \mathbf{A}_{SR,k} (-\mathbf{u}_{R,k} - \mathbf{\Omega}_k \Psi_{R,k} - \mathbf{r}_{RL,k} \mathbf{i}_{R,k});$$

$$(11) \quad \frac{d\mathbf{i}_{R,k}}{dt} = \mathbf{A}_{RS,k} (\mathbf{u}_{S,k} - \mathbf{r}_{S,k} \mathbf{i}_{S,k}) + \mathbf{A}_{R,k} (-\mathbf{u}_{R,k} - \mathbf{\Omega}_k \Psi_{R,k} - \mathbf{r}_{RL,k} \mathbf{i}_{R,k}) + \mathbf{\Omega}_k \mathbf{i}_{R,k};$$

$$(12) \quad \frac{d\omega_{1,k}}{dt} = \frac{1}{J_{1,k}} (c_{1,2,k} (\gamma_{2,k} - \gamma_{1,k}) + v_{1,2,k} (\omega_{2,k} - \omega_{1,k}) + M_{EM,k});$$

$$(13) \quad \frac{d\omega_{2,k}}{dt} = -\frac{1}{J_{2,k}} (M_{P,k} - c_{1,2,k} (\gamma_{2,k} - \gamma_{1,k}) - v_{1,2,k} (\omega_{2,k} - \omega_{1,k}));$$

$$(14) \quad \frac{dQ_k}{dt} = \frac{1}{L_{\Sigma,k}} (\rho_k g (H_{G,k} - S_{0,k} Q_k^2) - R_{\Sigma,k} Q_k);$$

where \mathbf{A}_{ij} – matrix, matrix which elements depend on the inverse inductance of the transformer and motor, $\mathbf{\Omega}$ – matrix of the rotor angular speed [1].

$$(15) \quad \frac{d\mathbf{V}}{dt} \equiv \frac{d\mathbf{u}_C}{dt} = \frac{1}{C} \mathbf{i}_C;$$

The stationary link between generalized speeds is determined by equations for the holonomic system:

$$(16) \quad \mathbf{i}_{SA,1} + \mathbf{i}_{SA,2} + \dots + \mathbf{i}_{SA,M} + \mathbf{i}_C - \mathbf{i}_{20} = 0.$$

$$(17) \quad \frac{d\mathbf{V}}{dt} = \frac{1}{C} (\mathbf{i}_{20} - \mathbf{i}_{SA,1} - \mathbf{i}_{SA,2} - \dots - \mathbf{i}_{SA,M}).$$

The angular speed equation of generalized discrete shaft units [1]:

$$(18) \quad \frac{d\gamma_{1,k}}{dt} = \omega_{1,k}, \quad \frac{d\gamma_{2,k}}{dt} = \omega_{2,k} \quad k = 1, 2, \dots, M$$

The electromagnetic torque of an asynchronous motor is calculated using [1]:

$$(19) \quad M_{E,k} = \sqrt{3} p_{0,k} (i_{SB,k} i_{RA,k}^{\Pi} - i_{SA,k} i_{RB,k}^{\Pi}) / \tau_k$$

where Π – indicates a transformed system of diagonal coordinates [1].

The hydraulic moment of the pumping system is determined from the equation [11]:

$$(20) \quad M_{P,k}(Q_k) = \frac{\rho_k g Q_k (H_{G,k} + S_{0,k} Q_k^2)}{\omega_{2,k}}$$

Differential equations system (7) – (14), (17), (18) is integrated including expressions (16), (19), (20).

Computer simulation results

A computer simulation was made for the electrohydraulic system. The system is shown in figures 1 and 2. The primary winding of the TOc 4000/35 power transformer was supplied by a source of infinite power and rated voltage 35kV. The ratings for the deep bar motor 12-52-8A are as follows: $P_N = 320$ kW, $U_N = 6$ kV, $I_N = 39$ A, $\omega_N = 740$, s^{-1} , $p = 4$, $J_R = 49$ kg · m². The other parameters are: $r_S = 1,27$ Ω, $R_{RL} = 0,21$ Ω, $\alpha_S = 38,9$ H⁻¹, $aRL = 70$ H⁻¹, $h = 0,038$ m, $l = 0,23$ m, $a = 0,005$ m. The motor magnetization curve is approximated by the equation: $\Psi_m = 12,4 \arctg(0,066i_m)$. The vertical pump type is OB 16-87. Four vertical pumps work with a gear ratio $k_T = 750/585$. It was assumed that the liquid heights of the pumps are: the first pump - 0 m, the second - 2 m, the third - 4 m and the fourth - 6 m. For each pump system, four variants of functional dependencies of load moments are approximated - see the expression (20): $M_{P,1}(\omega_{2,1}) = 0,624\omega^2$, $M_{P,2}(\omega_{2,2}) = 0,422\omega^2 + 24,407\omega$, $M_{P,3}(\omega_{2,3}) = 0,358\omega^2 + 38,297\omega$, $M_{P,4}(\omega_{2,4}) = 0,349\omega^2 + 47,653\omega$.

Compensation batteries with capacities $C_1=10\mu F$, $C_2=50\mu F$, $C_3=240\mu F$ were used to analyze transient states. Flexible couplings parameters were changed in the experiment. This had an effect on changing the own pumping systems frequency. The analysis was performed for the following own frequencies f_0 [5]:

- $f_0 = 26,5$ Hz,
- vibration beat before resonance – $f_0 = 44,9$ Hz,
- resonance – $f_0 = 48,5$ Hz,
- vibration beat after resonance – $f_0 = 53,4$ Hz,
- $f_0 = 61,6$ Hz.

The resonance state is achieved not for the synchronous frequency of 50 Hz, but for the asynchronous frequency in the analyzed system [5].

The following assumptions were made during the computer simulation:

- 1) All parameters of induction motors rotors were reduced to the stator winding side;
- 2) the primary winding of the power transformer has been brought to the secondary winding;
- 3) parameters of the mechanical system were reduced to the vertical pump with the gear.

After reaching the steady state, the power supply voltage of the power transformer was turned off.

Figures 3 and 4 show the transition phase A voltage and the phase A current. Phase A current flows through the compensation battery for the first experiment. Parameters of all couplings were selected in such a way that the own frequency of all four pump subsystems was 26,5 Hz. Analyzing the aforementioned drawings, it is possible to notice typical jumps of the analyzed functional dependencies. These changes are related to different load torques of motor depending on the water high value and incorrectly compensation battery selected. When starting all drives, the voltage drop is approx. 20 - 25% - figure 3,

which does not fully correspond to energy requirements. In Figure 4, the current consumed by the compensation battery is very small.

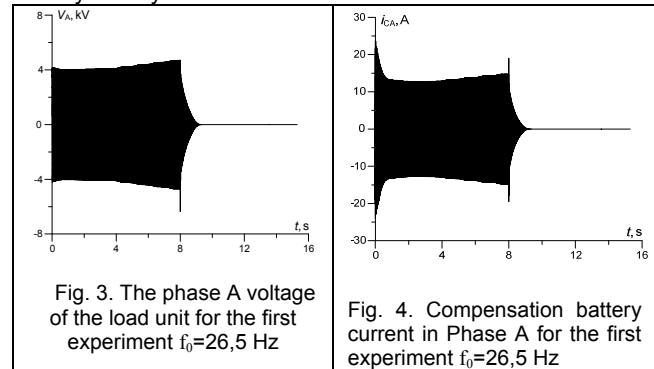


Fig. 3. The phase A voltage of the load unit for the first experiment $f_0=26,5$ Hz

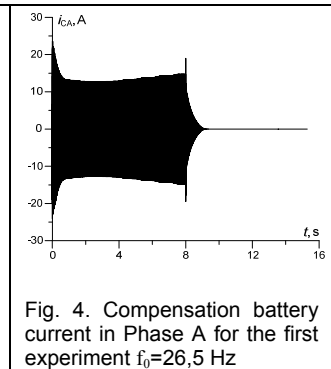


Fig. 4. Compensation battery current in Phase A for the first experiment $f_0=26,5$ Hz

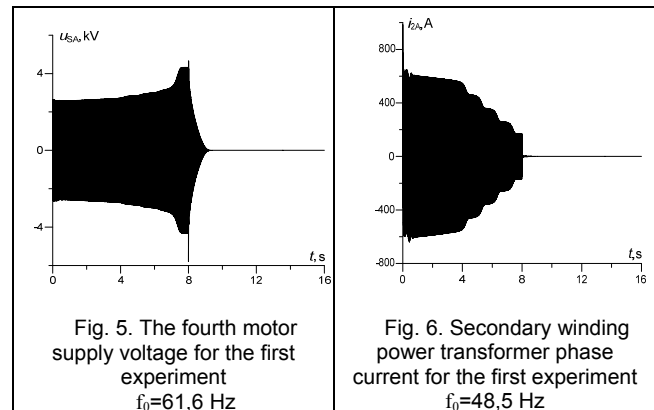


Fig. 5. The fourth motor supply voltage for the first experiment $f_0=61,6$ Hz

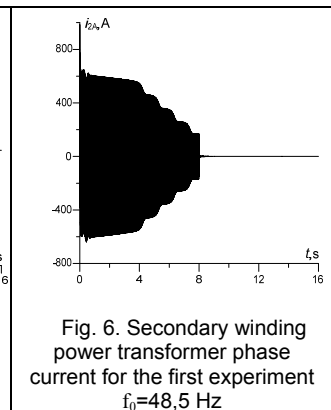


Fig. 6. Secondary winding power transformer phase current for the first experiment $f_0=48,5$ Hz

Figures 5 show the phase A supply voltage of the most loaded fourth motor. The own frequency of the pumps subsystems is 61,6 Hz. The phase current of the power transformer secondary winding at own frequency of 48,5 Hz was shown (fig. 6). It was for the first experiment of pump subsystems. The motor is powered by an air-core coil – figure 1. The air-core coil is necessary because there are frequent starts in the pump systems and, as a consequence, impact moments can cause damage to the pump vanes, especially in resonance and near-resonance states. Figure 6 shows the variability of the current of each pump drive associated with entering into the steady state.

Figure 7 shows the transient rotational speeds of all pump drives for the first experiment. Depending on the liquid height value, the start-up time of the drives increases, while the run-up time of the rotors decreases.

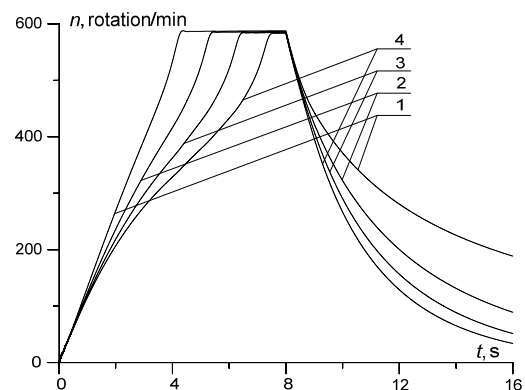


Fig. 7. Vertical pumps rotational speed for the first experiment $f_0=26,5$ Hz

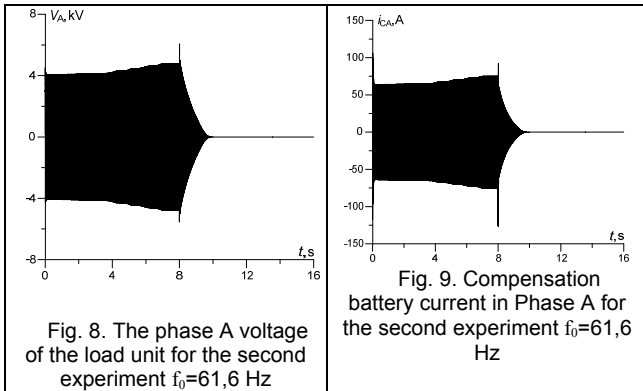


Fig. 8. The phase A voltage of the load unit for the second experiment $f_0=61,6$ Hz

Fig. 9. Compensation battery current in Phase A for the second experiment $f_0=61,6$ Hz

Figure 8 shows the transient supply voltage of phase A of the load unit. Figure 9 shows the phase current of the compensation battery. The voltage and current waveforms are the result of the second experiment for the 61,6 Hz own frequency. The energy situation is different in comparison to figures 3, 4. At the first, the start-up time of all drives has decreased. At the second unit supply voltage increased and the capacitor bank current increased almost five times. This is related to the increase the bank capacity for about 5 times. It should be noted that the compensation battery was selected correctly.

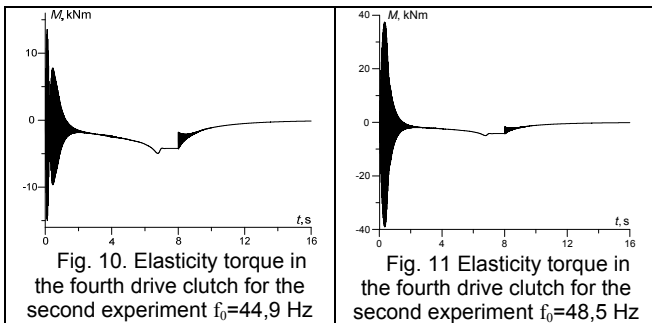


Fig. 10. Elasticity torque in the fourth drive clutch for the second experiment $f_0=44,9$ Hz

Fig. 11. Elasticity torque in the fourth drive clutch for the second experiment $f_0=48,5$ Hz

Figures 10 and 11 show transient elastic moments in the flexible coupling of the fourth pumping drive for the second experiment in emergency conditions: vibration beat before resonance - figure 10 and in the state of resonance - figure 11. The rated load torque for the fourth subsystem was about 4 kNm, and the shock torque reached 15 kNm before the resonance. This is the reason for faster wear of the clutch. The shock moment reaches 40 kNm in the resonant state. This causes failures in the pumping system.

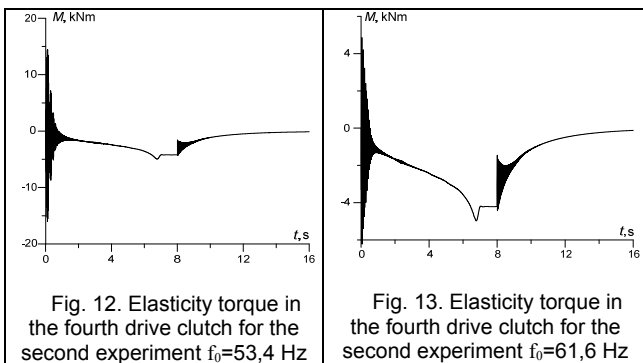


Fig. 12. Elasticity torque in the fourth drive clutch for the second experiment $f_0=53,4$ Hz

Fig. 13. Elasticity torque in the fourth drive clutch for the second experiment $f_0=61,6$ Hz

Figures 12 and 13 show the transient elastic moments in the flexible coupling of the fourth pump drive for the second experiment. This is the case in the state of vibrations after resonance and in the typical state of work. The first state is an emergency state, similar to that illustrated in Figure 10.

The second state is the working state. There is a small problem in the second state. The parasitic vibrations dumping is difficult for such an own frequency of the subsystem. Frequent starts and braking of pump drive increase the possibility of pump system failure.

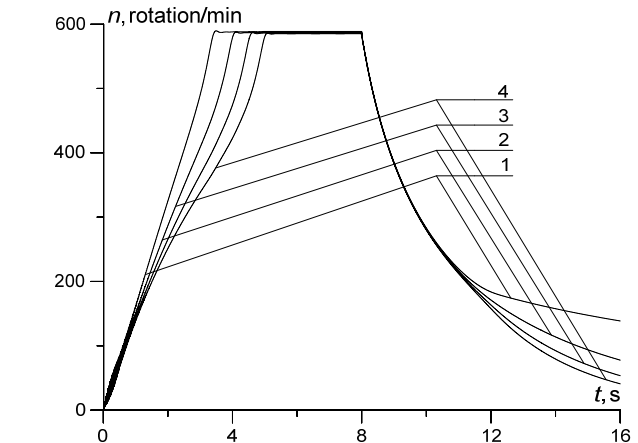


Fig. 14. Vertical pumps rotational speed for the third experiment at the resonance state $f_0=48,5$ Hz

Figure 14 shows the transient rotational speeds of all pump drives for the third experiment. In this case the capacity of the compensation battery is the maximum. All drives accelerated almost 70% faster compared to the first experiment. For the first consideration, it seems that the above-mentioned situation is very good for the load unit, because the transformer parameters were unchanged, and the start-up time of the motors was significantly decreased. But this way of thinking is incorrect, which is explicitly confirmed by the next two drawings.

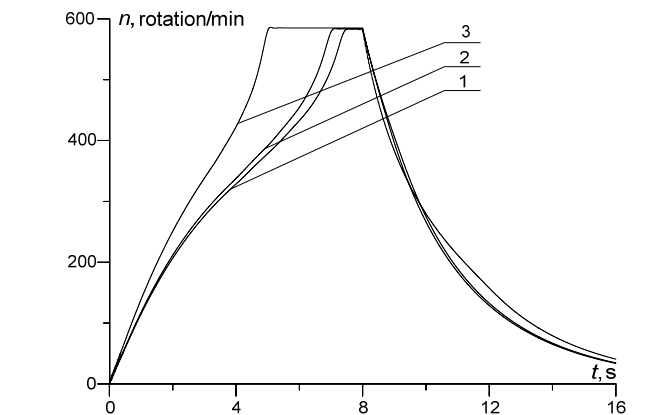
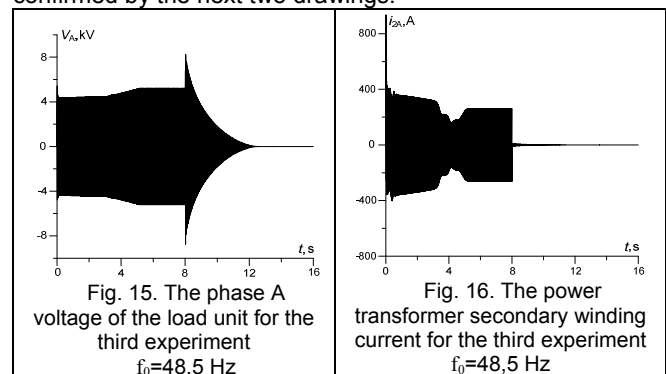


Fig. 15. The phase A voltage of the load unit for the third experiment $f_0=48,5$ Hz

Fig. 16. The power transformer secondary winding current for the third experiment $f_0=48,5$ Hz

Fig. 17. The fourth drive vertical pumps rotational speed for all three experiments $f_0=61,6$ Hz

Figure 15 shows transient phase A voltage of the load unit. Figure 16 shows the phase current A in the secondary winding of the power transformer. This is a third experiment

in resonant state case. On the base at figure 15 it can be concluded that the steady-state voltage is very high. This is an example of the too much reactive power compensation. It is clear that the concept of reactive power compensation is purely computational. From the applied physics point of view - the load unit voltage increases because capacity of the compensation battery is very high. The mentioned phenomenon is very dangerous for the power transformer. In this case, currents are very high (fig. 16).

Figure 17 shows the transient rotational speeds of the fourth pumping drive for all three experiments at the own frequency of all 61,6 Hz. The principles of load voltage stabilization described above are clearly visible here. For low-capacity batteries (curve 1), start of the most-loaded fourth drive takes the longest time. As the capacity of the compensation battery increases, the start-up becomes faster. And for maximum capacity, starting the drives is the fastest. Curve 2 - second experiment and curve 3 - third experiment.

Conclusions

1. The application of variational approaches to the construction of mathematical models of complex dynamic systems gives the opportunity to significantly expand the range of specialists in mathematical modeling. This becomes possible thanks to the interdisciplinary energy approach.

2. Mathematical modeling of pumping systems should be ultimately performed taking into account a wide range of physical influences. In this case, consideration is given to the final power output of the power supply transformer, the subcomponents of sophisticated movement transmission, dynamic thrusts and other.

3. An important element in the construction of dynamic models is the correctness of creating a non-conservative extended system lagrangian. This is the way to fully take into account the complex principles of electromechanical energy conversion in the load unit taking with other influences. In this case hydrodynamics influence are considered.

4. Based on the results of the computer simulation, the conclusions are as follows:

- parallel connection of few capacitors in compensation bank gives the possibilities to change capacity and gives opportunity to significantly improve the energy situation in the entire facility. This case gives the possibilities to reactive power control in the steady states.

- The correct choice of parameters of flexible couplings is a very important element of the analysis of asynchronous drives at the design process. Disregarding these principles may lead to emergency situations. It is possible to damage great power system in resonant states - in general.

- The start-up should be carried out at the maximum battery capacity (so-called starting capacity) in systems

equipped with a variable capacity compensation battery. After the start-up of the drives, progressively disconnect the capacitors. In the steady state, secure the most qualitative voltage characteristics, i.e., maximally efficiently compensate reactive power.

Author: dr inż. Andrzej Szafraniec, Kazimierz Pulaski University of Technology and Humanities in Radom, Faculty of Transport and Electrical Engineering, ul. Malczewskiego 29, 26-600 Radom, E-mail: a.szafraniec@uthrad.pl

REFERENCES

- [1] Czaban A., Zasada Hamiltona-Ostrogradskiego w układach elektromechanicznych, *Wydawnictwo T. Soroki*, Lwów 2015, 464
- [2] Czaban A., Lis M., Popenda A., Patro M., Nowak M., Model matematyczny zespołu elektrycznego składającego się z transformatora mocy, silników indukcyjnych, obciążenia nieliniowego RL oraz baterii kompensacyjnej, *Przegląd Elektrotechniczny*, 2015, Nr. 1, 129 – 132
- [3] Zhang D., Shi W., Chen B., Guan X., Unsteady flow analysis and experimental investigation of axial-flow pump, *Journal of Hydrodynamics*, 2010, v. 22(1), 35-43
- [4] Szafraniec A., Mathematical model of a drive system with synchronous motors and vertical pumps, *E3S Web of Conferences 84, nr 02015*, eISSN 2267-1242
- [5] Szafraniec A., Modelowanie matematyczne procesów oscylacyjnych w napędzie elektrohydraulicznym o podatnej transmisji ruchu, *Przegląd Elektrotechniczny*, R. 93 NR 12/2017, 167-170
- [6] Czaban A., Rusek A., Lis M., Popenda A., Lis T., Mathematical Modeling of Induction Generator Electrical Circuits using Hamilton's Formalism, *Proceedings of the 8th International Scientific Symposium on Electrical Power Engineering ELEKTROENERGETIKA 2015* September 16–18, 2015, Stará Lesná, Slovak Republic, 435-438
- [7] Lis M., Szafraniec A., Model matematyczny synchronicznego układu pompowego o podatnej transmisji ruchu, *Maszyny Elektryczne - Zeszyty Problemowe*, nr 2/2018, 165 – 170
- [8] Czaban A., Lis M., Mathematical modeling of transient states in a drive system with a long elastic element, *Przegląd Elektrotechniczny*, 88 (2012), nr 12b, 167-170
- [9] Łukasik Z., Czaban A., Szafraniec A., Żuk V., The mathematical model of the drive system with asynchronous motor and vertical pump *Przegląd Elektrotechniczny*, R. 94 NR 1/2018, 133-138
- [10] Sieklucki G., Orzechowski T., Sykulski R., Model matematyczny napędu z silnikiem indukcyjnym – metoda DTC-SVM, *Elektrotechnika i Elektronika*, 29, (2010) nr 1-2, 33-39
- [11] Mandrus W., Żuk W., *Hydraulika, napędy hydrauliczne i pneumatyczne maszyn wojskowych, ACB*, Lwów, (2013), 372
- [12] Ortega R., Loria A., Nicklasson P.J., Sira-Ramirez H., *Passivity-Based Control of Euler-Lagrange Systems: Mechanical, Electrical and Electromechanical Applications*. Springer Verlag, London 1998, 543